INT. J. REMOTE SENSING, 1988, VOL. 9, NO. 3, 447–467

# Intercomparison of satellite-derived cloud analyses for the Arctic Ocean in spring and summer

K. McGUFFIE†, R. G. BARRY‡, A. SCHWEIGER‡,
D. A. ROBINSON§ and J. NEWELL‡

† Department of Geography, University of Liverpool, Liverpool, England

‡ Cooperative Institute for Research in Environmental Sciences and Department of Geography, University of Colorado, Boulder, Colorado, U.S.A.

§ Lamont-Doherty Geological Observatory of Columbia University, Palisades, New York, U.S.A.

*(Received 5 February 1987; in final form 10 July 1987)*

**Abstract.** Several methods of deriving Arctic cloud information, primarily from satellite imagery, have been intercompared. The comparisons help in establishing what cloud information is most readily determined in polar regions from satellite data analysis. The analyses for spring–summer conditions show broad agreement, but subjective errors affecting some geographical areas and cloud types are apparent. The results suggest that visible and thermal infrared data may be insufficient for adequate cloud mapping over some Arctic surfaces.

## 1. Introduction

There is wide recognition of the importance of accurate global cloud cover data for climate research (Schiffer and Rossow 1983) and efforts to determine the character of global cloud cover go back many decades (MacDonald 1938). Cloud observations describe the fractional coverage of the sky (as observed from a point or, in the case of satellite data, for a particular area), the appearance of the cloud (stratiform, cumuliform) and height of the cloud base above the surface (see, for example, World Meteorological Organization 1956). Cloud type is determined for three levels, low, middle and high cloud. None of the existing global cloud climatologies provides comprehensive information for the polar regions. Of the 15 distinct global cloud climatologies reviewed by Hughes (1984), only two (Beryland and Strokina 1980, Sherr *et al.* 1968) provide information about both poles while a further four have information for one or other of the poles.

Polar cloud cover may play an influential role in ice-albedo feedback (Barry *et al.* 1984 b), which remains a crucial issue in the concern over $CO_2$ (and other greenhouse gas) global warming effects. Shine and Crane (1984) used a thermodynamic sea ice model to show that changes in Arctic cloudiness can have a marked effect on sea ice conditions. It is therefore desirable that the character of Arctic cloud be more reliably established. The most comprehensive cloud climatologies for the Arctic, by Vowinckel (1962), Huschke (1969) and Gorshkov (1983), are derived primarily from surface observations. They show a broad agreement over much of the Arctic in regard to the seasonal cycle of total cloud amount, namely a winter minimum and a summer maximum, as illustrated by Huschke's data in figure 1. However, there is less agreement between the climatologies regarding the geographical distribution of cloud cover, particularly in the case of low cloud in winter. As noted by Crane and Barry

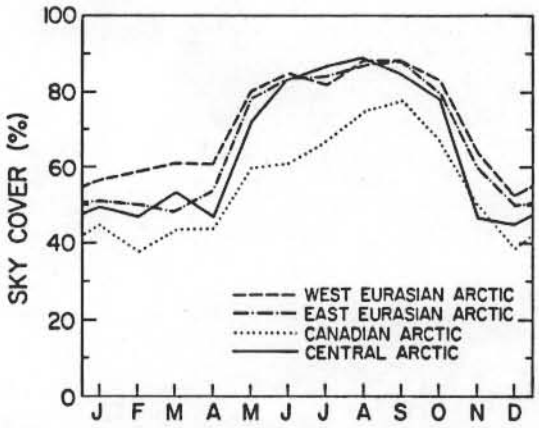


Figure 1. Annual variation of total cloud amount in four sections of the Arctic (from Huschke 1969).

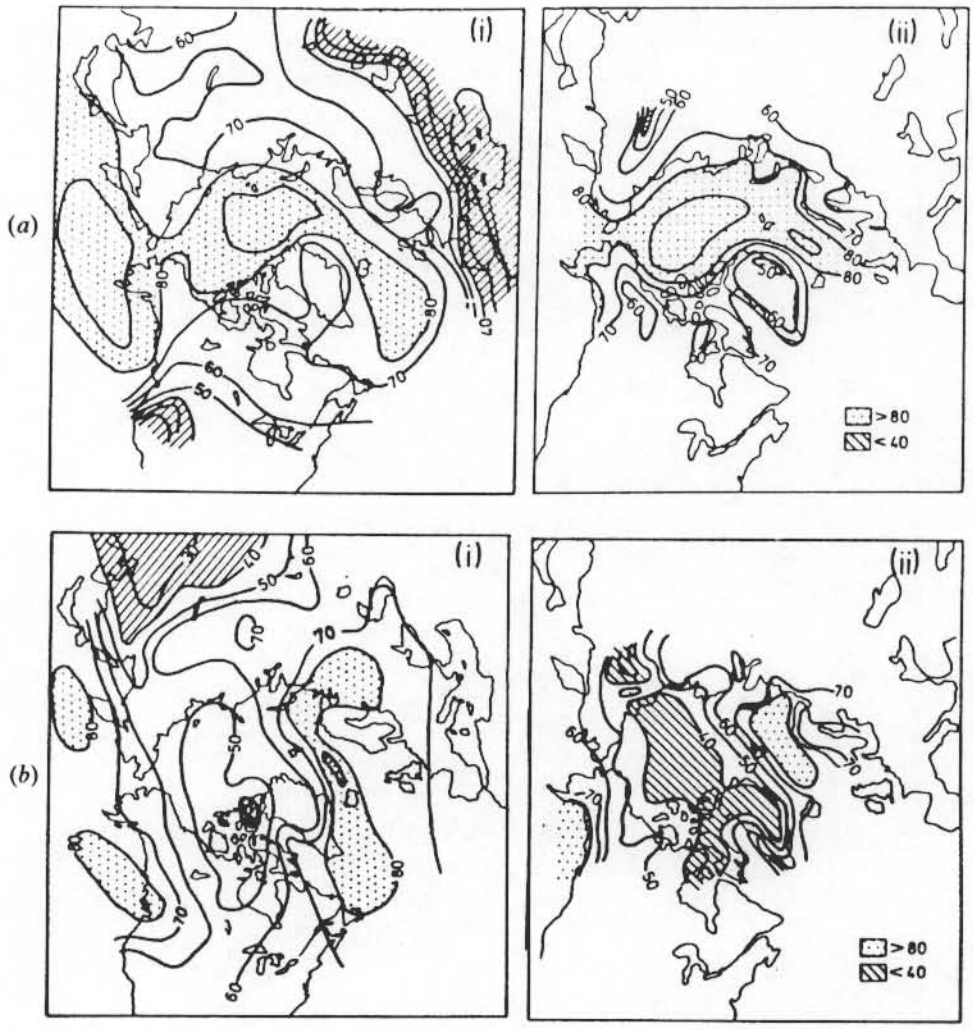


Figure 2. Mean total cloud amount (per cent) over the Arctic in (*a*) July (*b*) January according to (i) Beryland and Strokina (1980) and (ii) Vowinckel (1962).

(1984), for example, Voskresenskiy and Chukanin (1959) show a much lower frequency of occurrence of low clouds over the central Arctic Basin than does Vowinckel (1962). There are also considerable differences between the mean maps of total cloud for January and July presented by Vowinckel (1962) and those of Berlyand and Strokina (1980) (figure 2). This may be due in part to the incorporation in the latter source of some satellite observations.

Prior to the advent of satellites there were few observational studies of Arctic cloud. There were no meteorological stations in the Canadian Arctic Archipelago and northern Greenland until the late 1940s and, at most, there are only two or three drifting stations on the pack ice at any one time. Moreover, accurate reporting of cloud in the Arctic presents special problems for the observer. Loewe (1935, cited by Putnins 1970) noted that cloud observations in Greenland were not very precise, especially during the polar night. Ice crystal precipitation may occur even in the absence of cloud (Astapenko 1960). Even with present-day satellite radiance measurements, cloud cover determination in polar regions remains difficult due to the overall similarity of signatures over clouds and snow or ice in both visible and infrared wavelengths.

This study uses the results of three independent satellite-based analyses of Arctic cloud conditions for selected periods in spring and summer. The cloud cover maps were prepared using different techniques to identify and classify cloud, but all of the results were primarily derived from Defense Meteorological Satellite Program (DMSP) images. The scope of the intercomparison is determined by the availability of overlapping time intervals analysed in the various studies. Although somewhat limited, there is sufficient overlap to provide useful intercomparisons.

## 2. Analysis techniques

In this section we review the techniques used in the individual cloud analyses (termed nephanalyses) as a prelude to the comparison of their results. Of the three techniques which are discussed here, two are manual nephanalyses and the third is a computer-based automatic algorithm. The table summarizes the data sources and mapping techniques.

The automated algorithm is the US Air Force 3D-nephanalysis which has been described by Fye (1978) and more briefly in Hughes and Henderson-Sellers (1985). It categorizes cloud cover fraction and cloud level over the northern hemisphere on a $46 \times 46$ km grid. Over areas of snow and ice cover it is largely based on infrared imagery and surface station data. Each $46 \times 46$ km grid box contains 64 'pixels' which are reduced statistically to a single output every 3 hours (see Hughes and Henderson-Sellers 1985). Modes are identified in the frequency distribution of infrared counts and used to establish up to four clusters with thermally similar characteristics. An infrared radiance temperature is determined for each cluster and used to decide on the presence of cloud/no cloud based on a threshold method. The number of cloudy elements (5·5 km) over the 46 km grid is then established and an average value assigned to that grid point. Finally, surface and aircraft observations are integrated with the satellite data, together with a continuity field comprising data from the previous analyses, to fill in missing values. McGuffie (1985) uses the full spatial and temporal resolution of the 3D-neph data for the analyses reported here.

Technique 2 uses a manual classification of cloud characteristics for 3-day intervals during April–June in both 1979 and 1980 for areas north of 70°N. The 3-day interval sampling is considered to be sufficient to indicate the overall cloud climatology, given the persistence of Arctic weather systems. Additional dates were also analysed to

Characteristics of the data sources and classification procedures used for the three cloud mapping techniques.

| | McGuffie 1985 | Barry *et al.* 1986 | Robinson *et al.* 1985 |
|---|---|---|---|
| Data source | 3D-neph product from DMSP visible and IR digital data | DMSP visible and IR mosaic images | DMSP visible and IR orbital images |
| Pixel resolution | 5·5 km | 5·4 km | 2·7 km (supplementary 0·6 km) |
| Data sampling grid interval | ~45 km | ~42 km (digitized from analysed cloud maps) | ~190 km |
| Temporal sampling | 3-hourly data | ~3-day | ~3-day |
| Cloud identification criteria | Cloud/no-cloud threshold set by histogram analysis of visible and IR values over 64 pixels. Grid point cloud fraction is box-averaged value | Visual recognition (1) cloud-free areas, stratiform/cumuliform areas from visible image (2) low/middle/high cloud levels from IR relative grey scale and evidence of cloud shadows | Visual recognition of cloud and surface features |
| Cloud classification | Total cover (per cent) (3D-neph also gives cloud type and estimated heights of base and top) | Cloud/cloud-free for each level mapped for synoptic and mesoscale features (typically $\geqslant \frac{1}{2}$–1° latitude in extent) | Cloud-free, thin/ moderate/thick cloud |

provide 10-day samples for each of eight mean sea-level pressure patterns identified by a computer classification, as discussed by Barry *et al.* (1986, 1987). Shortwave band (0·4–1·1 $\mu$m) DMSP images were used to identify areas of open conditions (largely cloud free), stratiform (flat, featureless) cloud and 'cumuliform' (cells or rolls with some vertical development showing texture on the images). Open conditions were identified particularly on the basis of lead patterns in the ice being visible. The infrared (10·5–12·5 $\mu$m) images were used, together with shortwave evidence of cloud shadows, to divide the cloud into low, middle or high categories according to relative grey scale. The 5·4 km resolution computer-rectified and gridded mosaic images allowed cloud covered areas of extent $\geqslant c.$ $\frac{1}{2}$°–1° latitude to be outlined. These maps were subsequently digitized as cloud covered or cloud free for the three levels at each point on a 42 × 42 km grid. The cloud type information was not analysed digitally and is not discussed further here. The low cloud amounts for the April monthly average and pressure-pattern average maps are weighted by 0·5 to eliminate an apparent bias in April caused by low Sun angle and Arctic haze effects. This is discussed more fully in Barry *et al.* (1987).

The second manual technique (Robinson *et al.* 1985, 1986 a) used available DMSP direct readout images with 0·6 km resolution for the Alaskan sector and 2·7 km resolution orbital strips elsewhere. Clouds were visually differentiated from snow and ice, primarily by the characteristic large-scale features of the pack ice fields identified in shortwave imagery. In addition, certain cloud fields, particularly those located in cyclonic regions, were recognized by their characteristic shapes and patterns. These

were often evident in both shortwave and infrared imagery. Three cloud categories were recognized: thin cloud (surface features clearly recognizable but with reduced contrast from cloud-free skies), moderate cloud (surface features marginally recognizable) and thick cloud. Cloud cover was charted at about 3-day intervals from mid-May to mid-August of 1977 and 1979 and digitized using a standard grid with an approximate grid interval of 190 km.

Specific intercomparisons of the categories used by Robinson *et al.* (1985) and Barry *et al.* (1986) for 24 June and 13 July 1979 suggest that thick corresponds to cloud areas with vertical development (cumuliform) and that moderate cloud would usually be stratiform cloud at the middle level. A check for sample days on the possible differences in interpretation that might arise as a result of using the 5·4 km rather than the 2·7 km resolution imagery suggests little or no effect for the categories of open or cumuliform cloud.

## 3. Intercomparison of results

We begin by examining the results for the monthly time scale. In general, the analyses show more cloud over the Subarctic than over the Arctic Ocean. McGuffie's data for May 1979 show that cloud decreases towards the pole with a slight increase again near the centre of the basin, a phenomenon which was also reported by Robinson *et al.* (1985). The zonal mean cloud amount determined by R.G. Crane (in Barry *et al.* 1984a) for May 1979 and May 1980, using a manual interpretation of large-scale features on DMSP imagery, also illustrates this tendency (figure 3). Although May 1980 appears to have been slightly more cloudy, the general pattern has remained the same. These results are all much lower than the climatology of Vowinckel (1962) who describes cloud as *increasing* from North America towards the pole in May and the other summer months, reversing the pattern of April. Possible reasons for this contradiction are discussed further below.

Figure 4 shows the geographical distribution from the 3D-nephanalysis and the manual interpretation of Barry *et al.* (1986) for the month of May 1979. The results for the 3D-nephanalysis in figure 4 (*a*) refer only to the common dates available from the manual analysis for May. The 3D-nephanalysis shows substantially less cloud over the Arctic than the manual analysis. In fact, the 3D-nephanalysis agrees better, in terms of

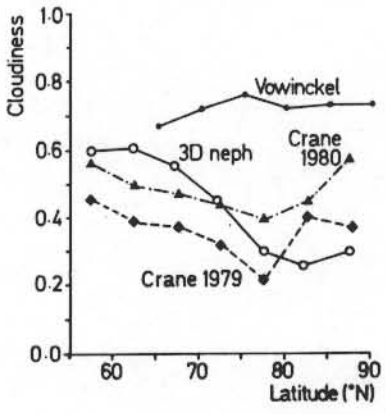


Figure 3. Zonal mean cloud amounts 58°–90°N in May showing mean values (Vowinckel 1962), manual analysis for 1979 and 1980 (Crane in Barry *et al.*, 1984a) and 3D-nephanalysis of 1979 (McGuffie 1985).

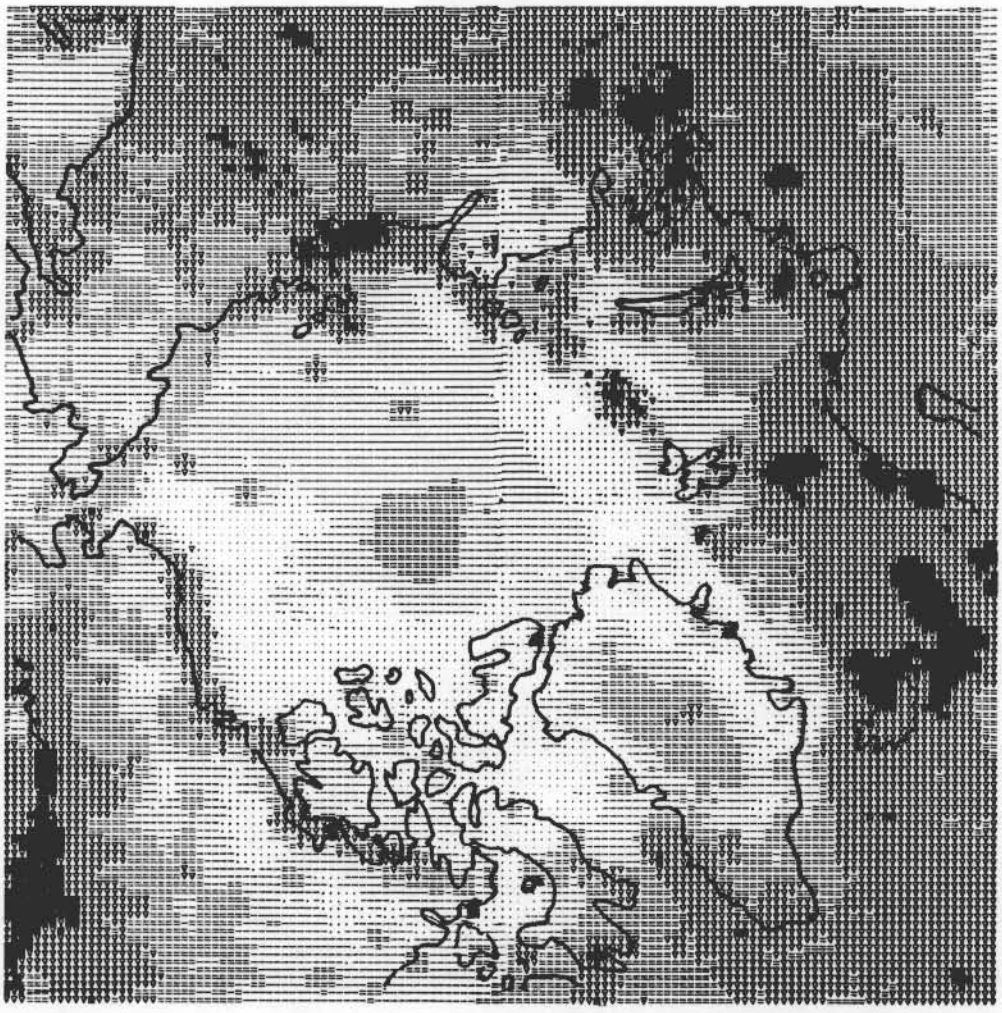


(*a*)

Figure 4. Mean total cloud amount for May 1979 (*a*) from 3D-nephanalysis data, per cent (McGuffie 1985), sampled at 3-day intervals and (*b*) from manual analysis of DMSP images at 3-day intervals; per cent (Barry *et al.* 1986), and (*c*) middle level cloud from the corresponding analysis to (*b*); per cent.

(*b*)

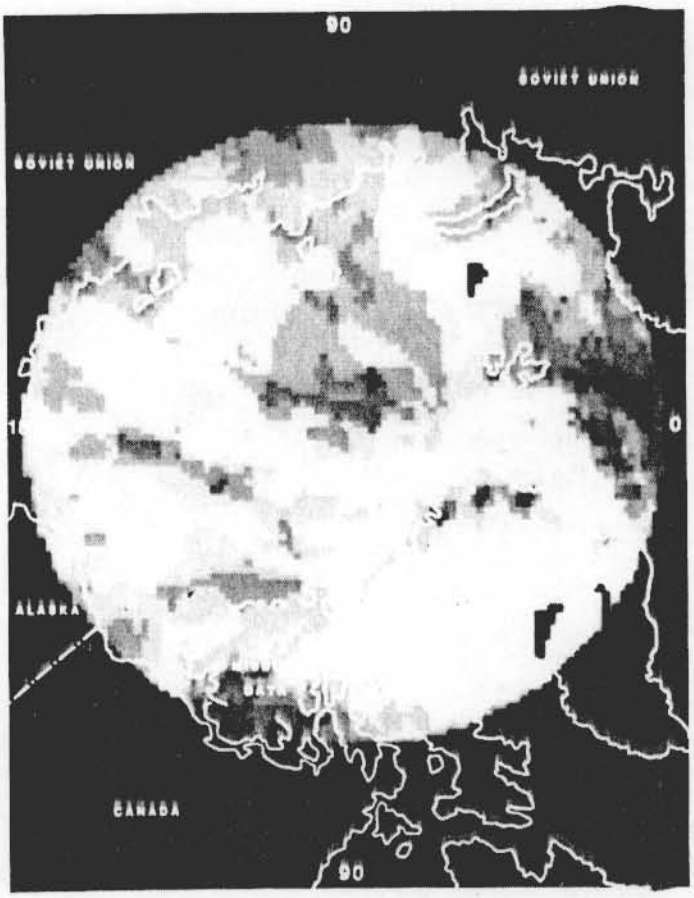
90
SOVIET UNION
SOVIET UNION
ALASKA
CANADA
90

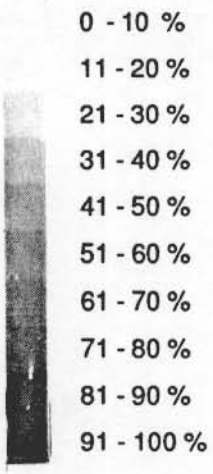
0 - 10 %
11 - 20 %
21 - 30 %
31 - 40 %
41 - 50 %
51 - 60 %
61 - 70 %
71 - 80 %
81 - 90 %
91 - 100 %

(*c*)

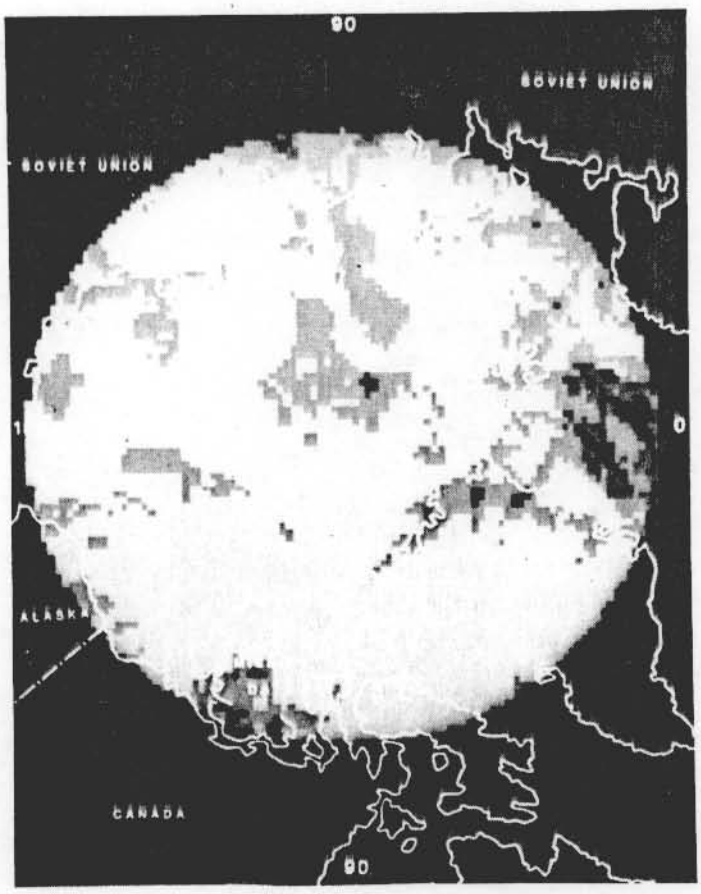
90
SOVIET UNION
SOVIET UNION
ALASKA
CANADA
90

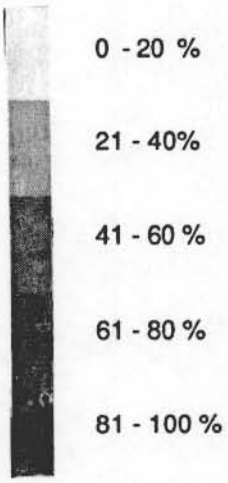
0 - 20 %
21 - 40%
41 - 60 %
61 - 80 %
81 - 100 %

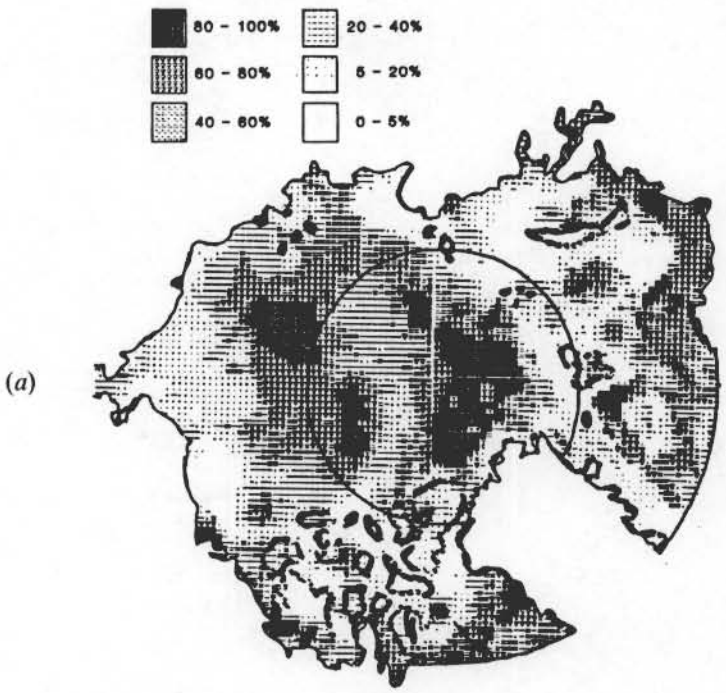


(*a*)

Figure 5. Total cloud amount over the Arctic for 10 April 1979 (*a*) from 3D-nephanalysis (McGuffie 1985) and (*b*) from manual analysis (for 9 April) (Barry *et al.* 1986), and (*c*) mean sea-level pressure analysis (millibars) for 10 April (Thorndike and Colony 1980).

cloud amount over the central Arctic, with the middle level cloud analysis of the manual technique (figure 4 (*c*)). This result is probably due to the temperature structure of the Arctic atmosphere in summer, when the near-surface layers are almost isothermal and only middle and higher-level clouds may be different enough in temperature to be separable from the ice surface. Both analyses agree that there is a cloudiness maximum over the North Atlantic Ocean, associated with cyclone activity. There is disagreement in the cloud cover over Greenland, where the 3D-nephanalysis reports a cloud maximum in opposition to the other retrieval. This may be due to the misidentification of the high ice plateau as cloud by the automated algorithm. The mean surface pressure map for May 1979 indicates a large anticyclone over northern Greenland which supports the case for a cloud-free area. Both analyses agree on the presence of a relatively cloud-free area between east Greenland and Spitzbergen but, in the Beaufort Sea, the 3D-nephanalysis shows less cloud than the manual technique.

Next, the results of the 3D-nephanalysis for individual daily cloud maps are compared with those of the manual technique of Barry *et al.* (1986) for April. On these maps, cloud data are not included from the 3D-nephanalysis over Greenland. The 12 GMT mean sea-level pressure maps from Thorndike and Colony (1980) incorporate measurements from 16 drifting buoys on the ice and up to 70 coastal and land stations. Figures 5–7 show a generally good agreement in the patterns of total cloud obtained by the 3D-nephanalysis and technique 2. In figure 5 for 10 April, 1979, with high pressure over Greenland and the central Arctic, both analyses show an area of cloud located over the pole and a relatively clear area north of the Arctic coastline, in the Barents Sea and around Greenland. In comparison with figure 5, which resembles the mean cloud pattern for April 1979, there is a very different cloud distribution for 15 April (figure 6 (*a*) and (*b*)). The pressure pattern features a high over the East Siberian

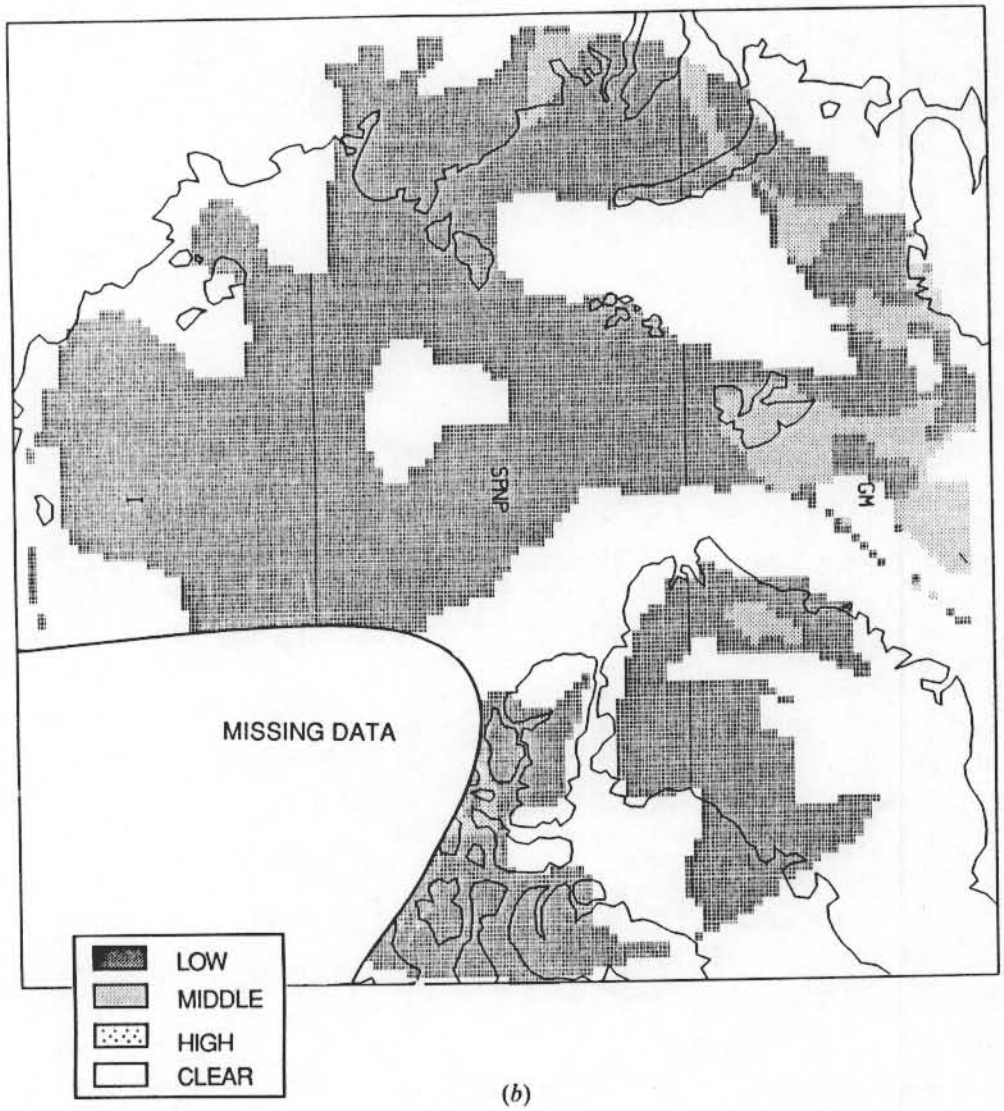
SRNP
GM
MISSING DATA
LOW
MIDDLE
HIGH
CLEAR

(*b*)

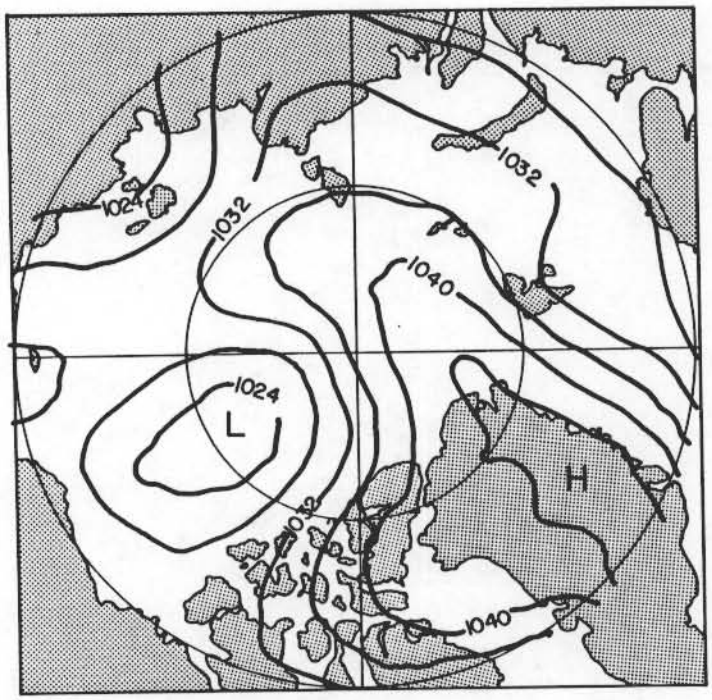
1032
1024
1032
1040
1024
L
H
1032
1040

(*c*)

(*a*)

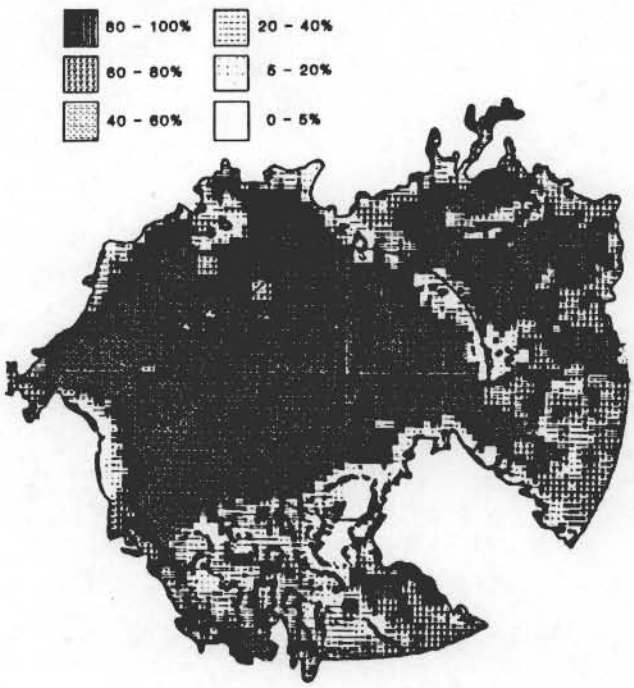


Figure 6. Total cloud amount over the Arctic 15 April 1979 (*a*) from 3D-nephanalysis (McGuffie 1985) and (*b*) from manual analysis (Barry *et al.* 1986), and (*c*) mean sea-level pressure analysis (millibars) for 15 April (Thorndike and Colony 1980).

Sea with easterly flow in the Barents Sea–Greenland sector. The Arctic Ocean has large amounts of cloud on both April maps. In this case most Arctic coastal stations would clearly be unrepresentative of the Arctic Ocean. The agreement between the analyses is weaker in figure 7 (*a*) and (*b*), for 25 April, respectively, in part due to the 1-day time difference between them. The low pressure system in the Beaufort Sea is represented by heavier cloud cover in the 3D-nephanalysis and the manual analysis, but there is substantial disagreement over the Siberian sector of the Arctic.

Overall, the cloud charts obtained by manual analysis show a reasonable agreement with the 3D-nephanalysis for the individual dates. One feature that appears to be common to both analyses of mean cloud for the month of April is the presence of a maximum of cloud cover over the central Arctic Ocean. However, the manual technique may exaggerate this due to the bias thought to be caused by pollution layers at a time of very low solar elevation angle (Barry *et al.* 1986).

Finally, comparison is made between the 3D-nephanalysis and the manual techniques of Robinson *et al.* (1985) for three dates in June 1979. Figure 8 for 10 June, characterized by a Kara Sea low and East Siberian–Beaufort Sea high, shows quite close agreement between the patterns obtained by Robinson *et al.* and the 3D-nephanalysis, although the amounts depicted by the latter are not as high as might be expected given the 'thick' cloud cover identified manually. Figure 9 for 13 June (East Siberian Sea high, central Arctic low) and figure 10 for 15 June (low over Ellesmere Island) refer to a low pressure system noted by Kukla (1984) that moved across the Pole from the Taymyr Peninsula to the Canadian Arctic Archipelago, and contributed to the onset of the summer snow melt regime on the pack ice. LeDrew (1987) analyses the dynamic properties and vertical motion of this system. Figures 9 and 10 show a considerable difference between the manual analyses and the 3D-nephanalysis. In both cases, the latter shows considerably less cloud over the Arctic Ocean. This probably

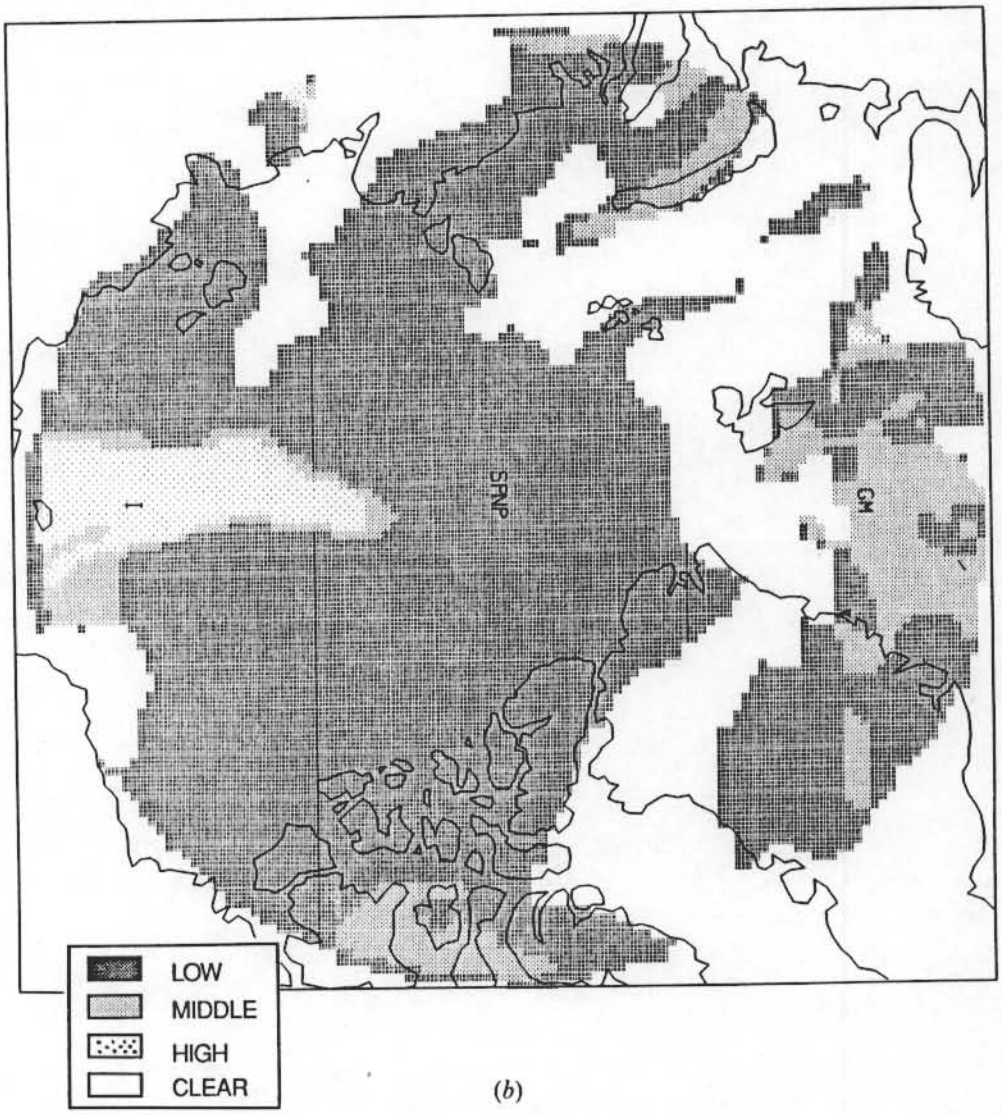
SPAIN
FRANCE
LOW
MIDDLE
HIGH
CLEAR

(*b*)

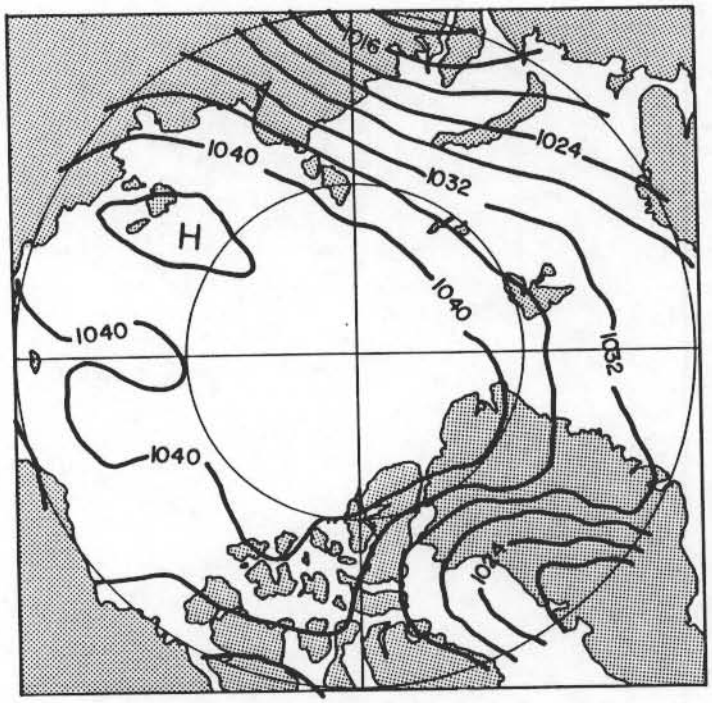
1016
1024
1040
1032
H
1040
1040
1032
1040

(*c*)

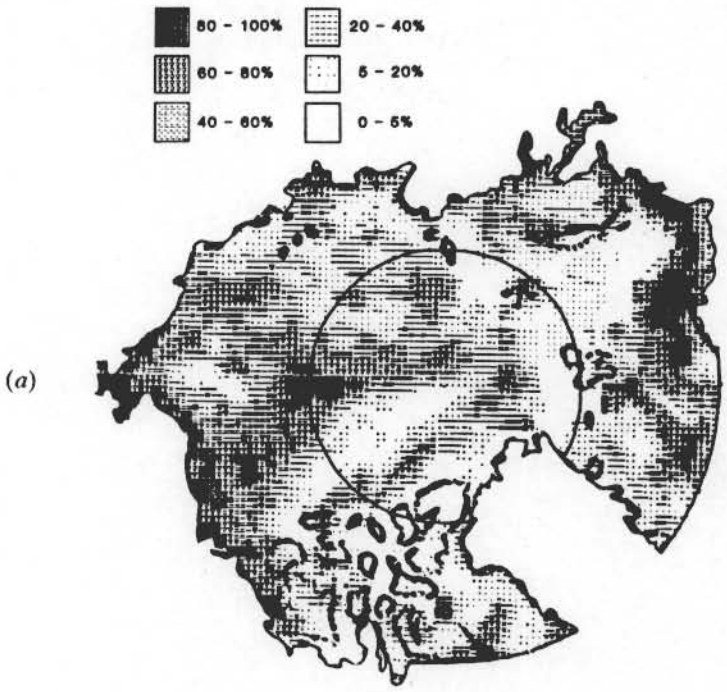


(*a*)

Figure 7. Total cloud amount over the Arctic 25 April 1979 (*a*) from 3D-nephanalysis (McGuffie 1985) and (*b*) from manual analysis (for 24 April) (Barry *et al.* 1986), and (*c*) mean sea-level pressure analysis (millibars) for 25 April (Thorndike and Colony 1980).

reflects the influence of the lower tropospheric temperature structure on the 3D-nephanalysis retrieval technique noted earlier. The two manual analyses for 15 June are in general in good agreement for the main cloud-covered areas (low or middle on figure 10 (*c*) corresponding with thick or medium on figure 10 (*b*)) and the areas of clear or high cloud (figure 10 (*c*)) and clear or thin cloud (figure 10 (*b*)). The analyses of Robinson *et al.* (1985) for both dates show cloud bands associated with the low pressure systems on figure 10 (*d*). Cloud models have been extensively developed for mid-latitude weather patterns (Carleton 1984, for example), but for the Arctic insufficient data are as yet available to establish reliable synoptic models (Fraser 1973).

## 4. Discussion and conclusions

This comparison of satellite-derived Arctic cloud information produced by two manual analysis techniques and 3D-nephanalysis (an automated algorithm) shows that these methods are capable of capturing broad climatological features of the cloud cover. However, the spatial patterns are subject to error due to surface effects that may mislead the interpreter or bias the algorithm. This variability makes it difficult to assign reliability estimates. None of the techniques discussed above has been able to portray all of the characteristics of Arctic cloud cover. The automated IR threshold techniques has problems in the Arctic because of the temperature structure of the lower atmosphere, with a persistent surface inversion and warmer low-level clouds in winter and a near-isothermal structure and extensive persistent stratiform clouds in summer. Manual analysis is subjective and depends on the skill of the analyst, with decisions as to the amount and nature of the cloud cover in complex situations inevitably differing between analysts.

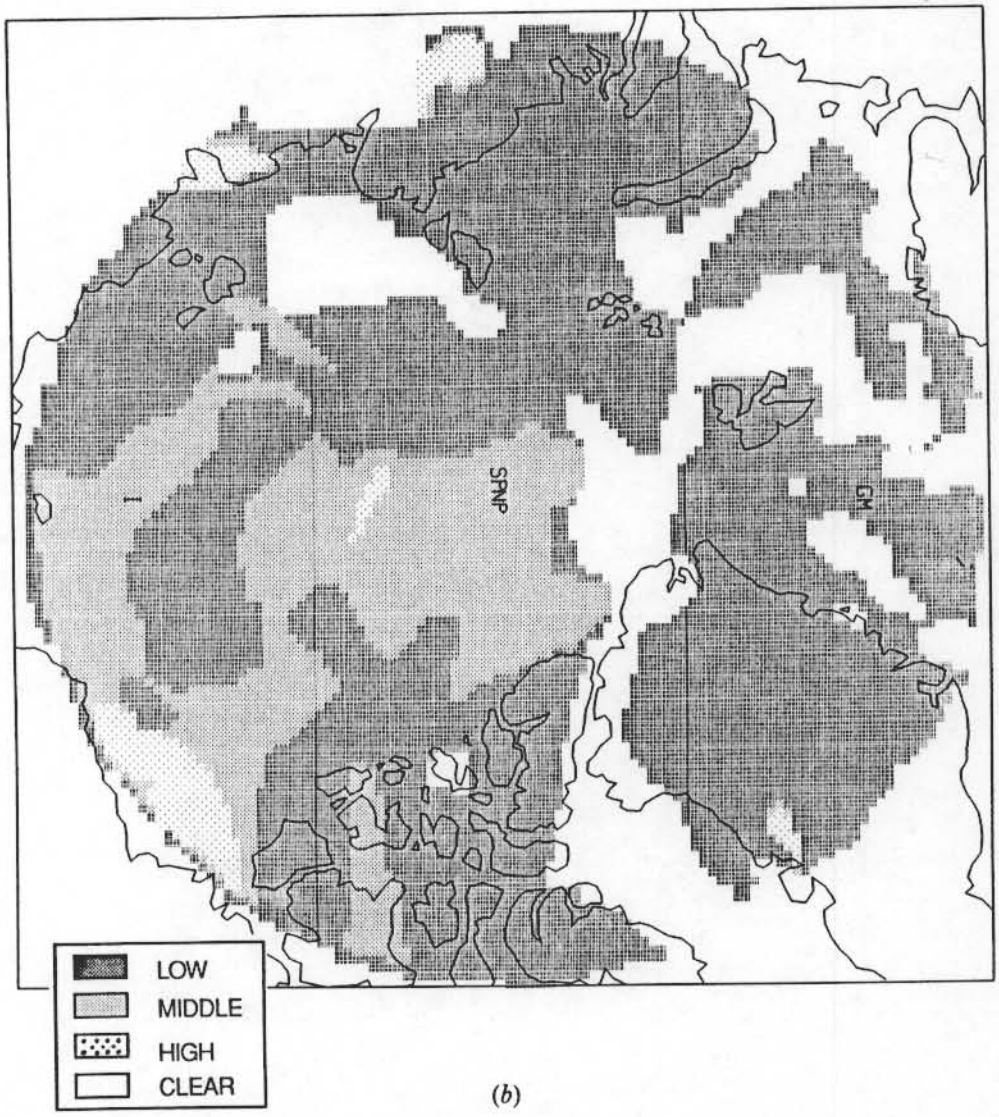


(*b*)

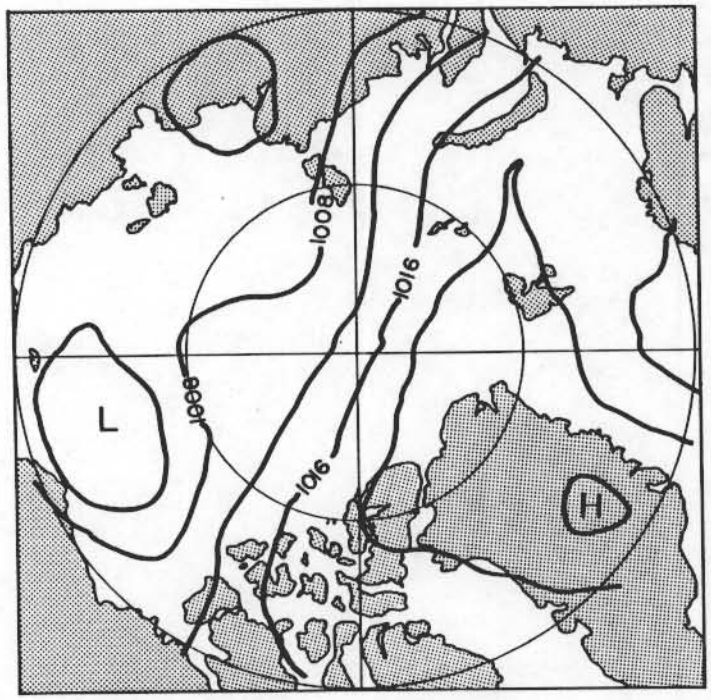


(*c*)

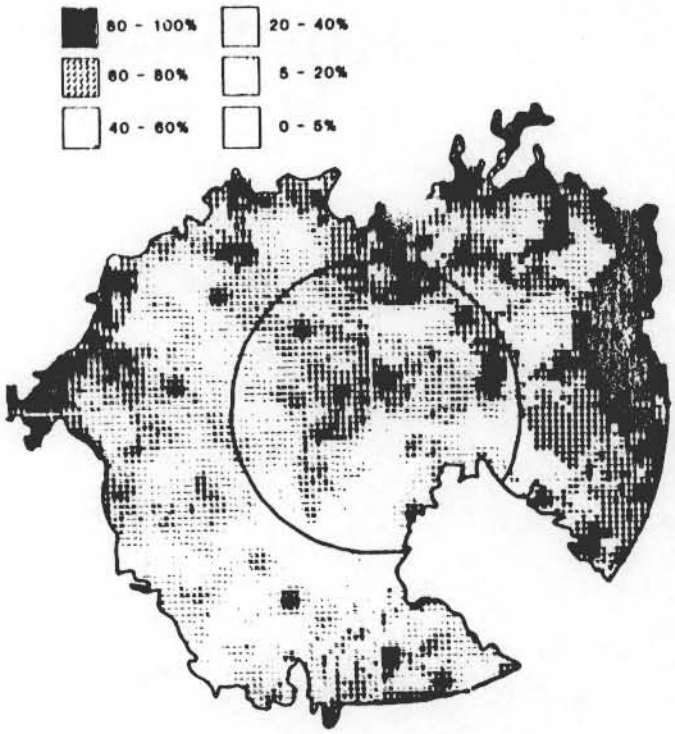


(*a*)

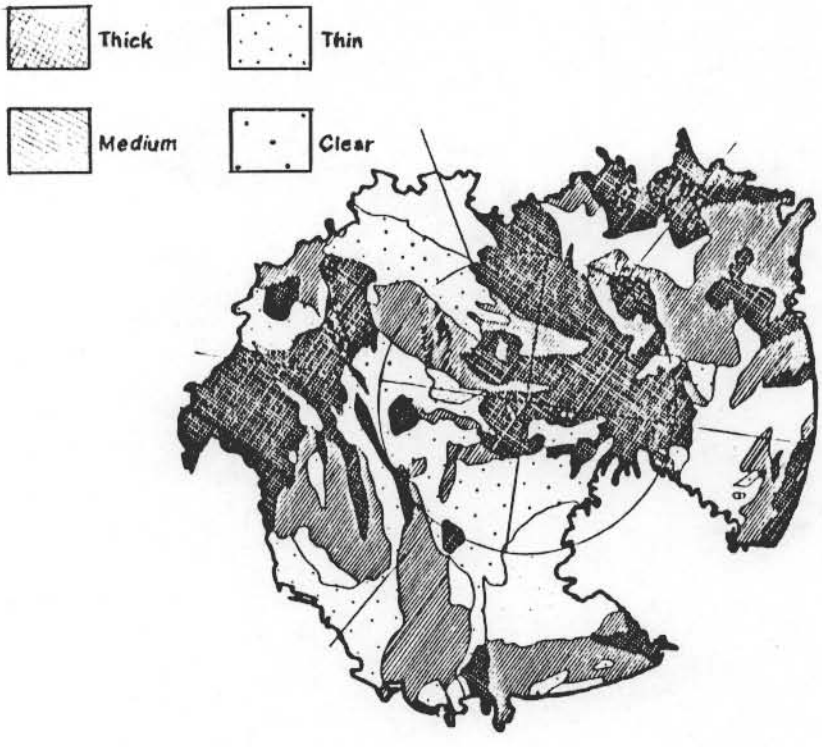


(*b*)

Figure 8. Total cloud amount for 10 June 1979 (*a*) from 3D-nephanalysis (McGuffie, 1985) and (*b*) from DMSP imagery analysis (Robinson *et al.* 1985), and (*c*) mean sea-level pressure analysis (millibars) for 10 June (Thorndike and Colony 1980).

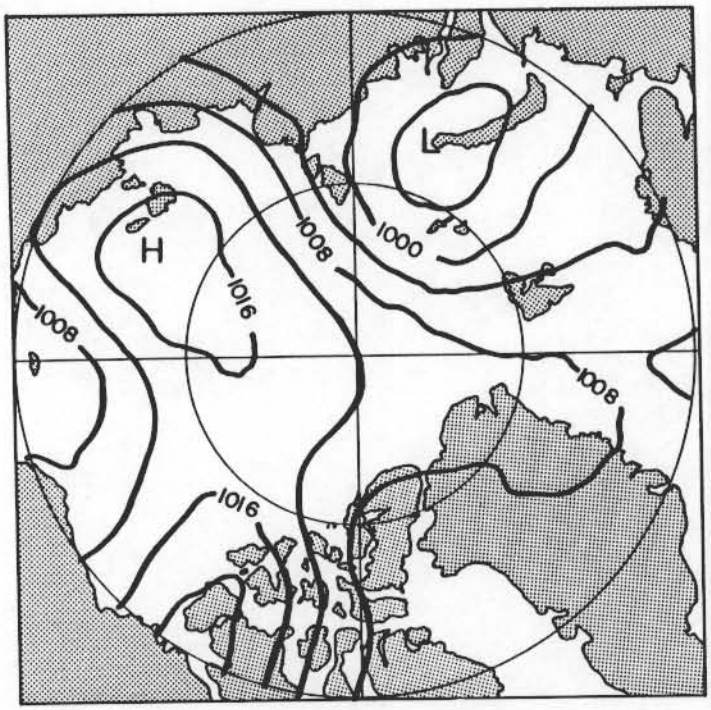


(*c*)

The estimates of Arctic cloudiness derived manually from satellite imagery are lower than those derived from surface observations, as noted elsewhere by other workers (Tanizer 1968, Malberg 1973). In part this reflects the statistical effect of the scale of resolution of the data (Henderson-Sellers *et al.* 1981). Station observations of cloud amount tend to be bimodal (presence, absence) whereas 5° grid boxes have a J-shaped frequency distribution. This difference also involves the consequences of what is often referred to as the 'observer seeing sides of clouds' problem. This bias may be exaggerated in the Arctic by the high albedo surface. The multiple reflection of shortwave radiation from clouds, and in spring from Arctic haze layers, will make it more difficult for the ground observer to identify breaks in the cloud. It seems likely that some of the difference between surface and satellite observations in the Arctic may be due to the background contrast viewed from the surface and from a satellite. A surface observer views a very low contrast, often milky blue sky, whereas the interpreter of satellite photos is often presented with the high contrast offered by leads in the ice cover. Calculations show that on clear days the presence of an aerosol layer can increase the downward diffuse radiation by up to 60 per cent. Consequently, a thin cloud layer over fractured sea ice may be recorded as broken cloud by a satellite image analyst and yet be reported as 100 per cent cover by an observer at the surface.

The results of the analyses also suggest that in the early part of the spring–summer season cloudiness is strongly influenced by weather systems. The melting of snow cover on the Arctic sea ice, which is in part initiated during May and June by large-scale warm air advection, is also associated with synoptic weather system activity (Robinson *et al.* 1986 b). This subsequently enables local advection over the melting ice surfaces to contribute to the increase in basin-wide cloudiness, particularly by the production of the widespread summer-time Arctic stratus clouds.

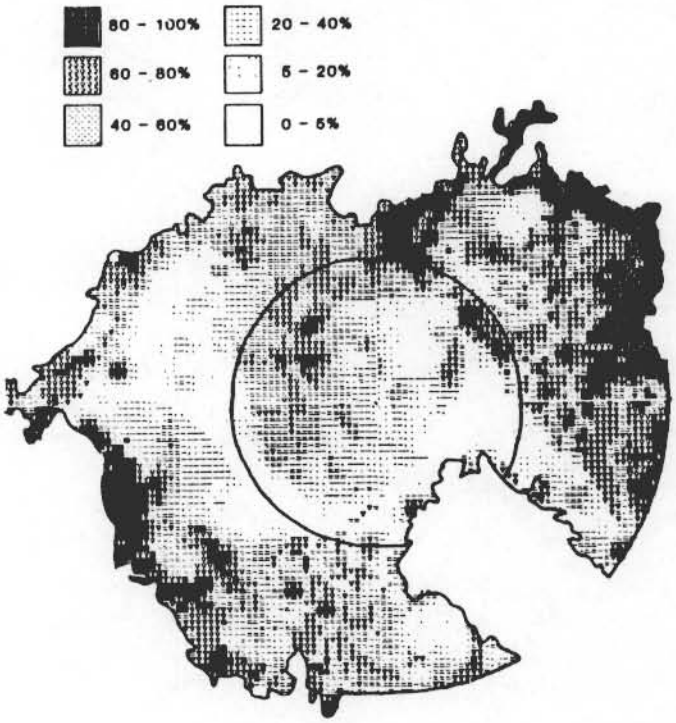


(*a*)

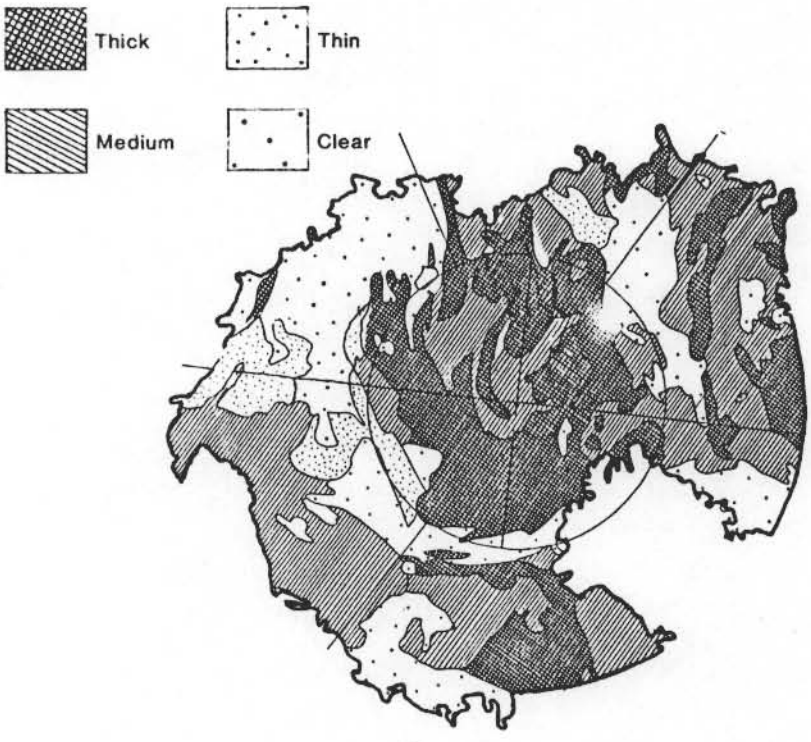


(*b*)

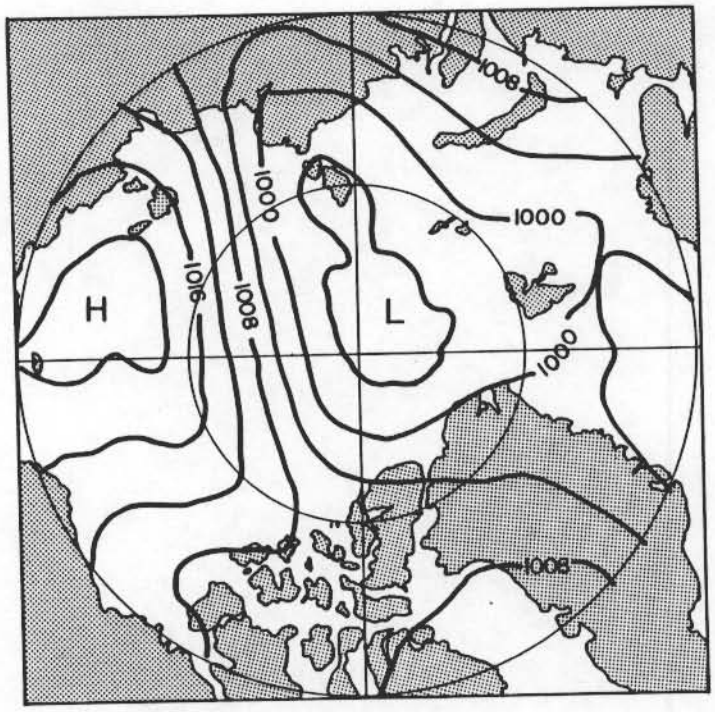


(*c*)

Figure 9. Total cloud amount for 13 June 1979 (*a*), (*b*) and (*c*) as for figure 8.

Changes in the atmospheric circulation and synoptic patterns, which are predicted to occur in response to increasing $CO_2$ concentrations for example, might be manifested by changes in cloudiness in spring. Such changes would affect the surface energy balance and most likely the timing of melt onset. Consequently, additional data on the occurrence of Arctic clouds and on their optical properties are urgently required if modelling studies of possible climate perturbations in the Arctic are to be successful. Satellites potentially offer the best way of deriving cloud parameters in the polar regions, but it remains for a consistent automatic classification procedure of high latitude clouds to be developed. Our results suggest that this probably cannot be achieved through the use of only visible and thermal infrared data. The manual techniques take into account surface features visually identifiable through thin or transient cloud cover. Over snow and ice, however, the 3D-nephanalysis algorithm scheme relies principally on the infrared channel as noted above. An improved automatic classification may need to incorporate these textural aspects of the scene, as well as employing a 1·6 or 3·7 $\mu$m channel to help resolve the mapping of low-level stratiform water cloud.

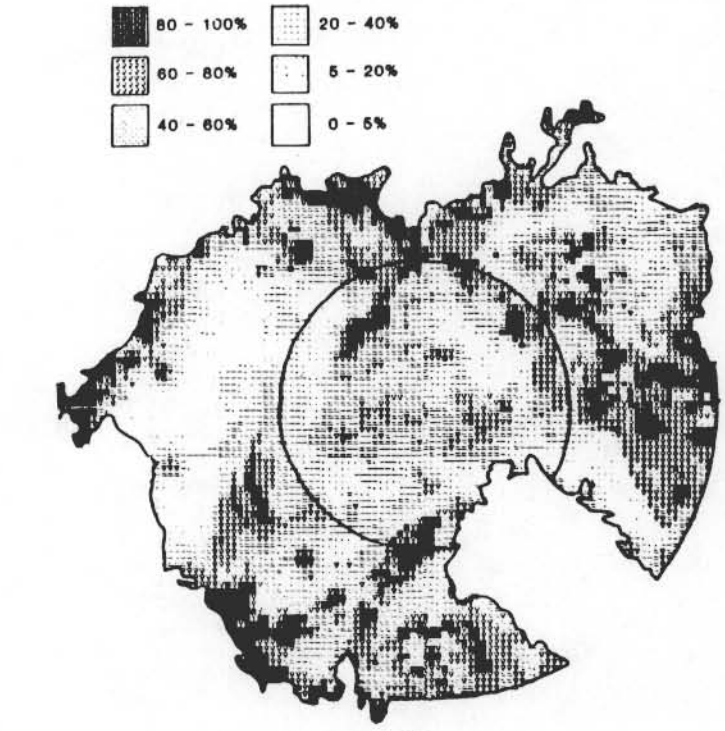


(*a*)

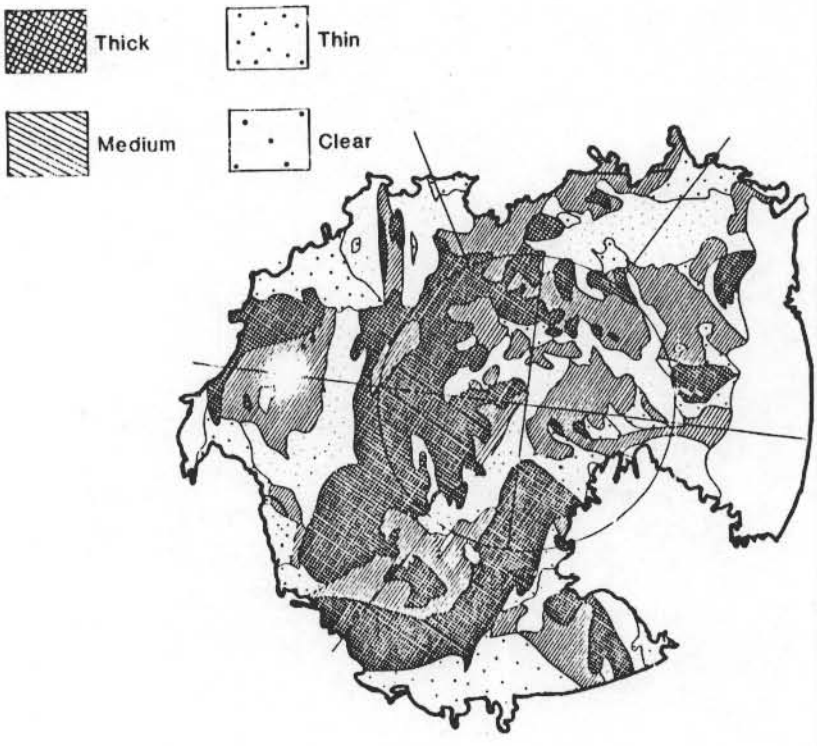


(*b*)

Figure 10. Total cloud amount for 15 June 1979, (*a*) and (*b*) as for figure 8 (the blank area in (*b*) in the North Atlantic represents missing data); (*c*) manual analysis (Barry *et al.* 1986) and (*d*) mean sea-level pressure analysis (millibars) for 15 June (Thorndike and Colony 1980).

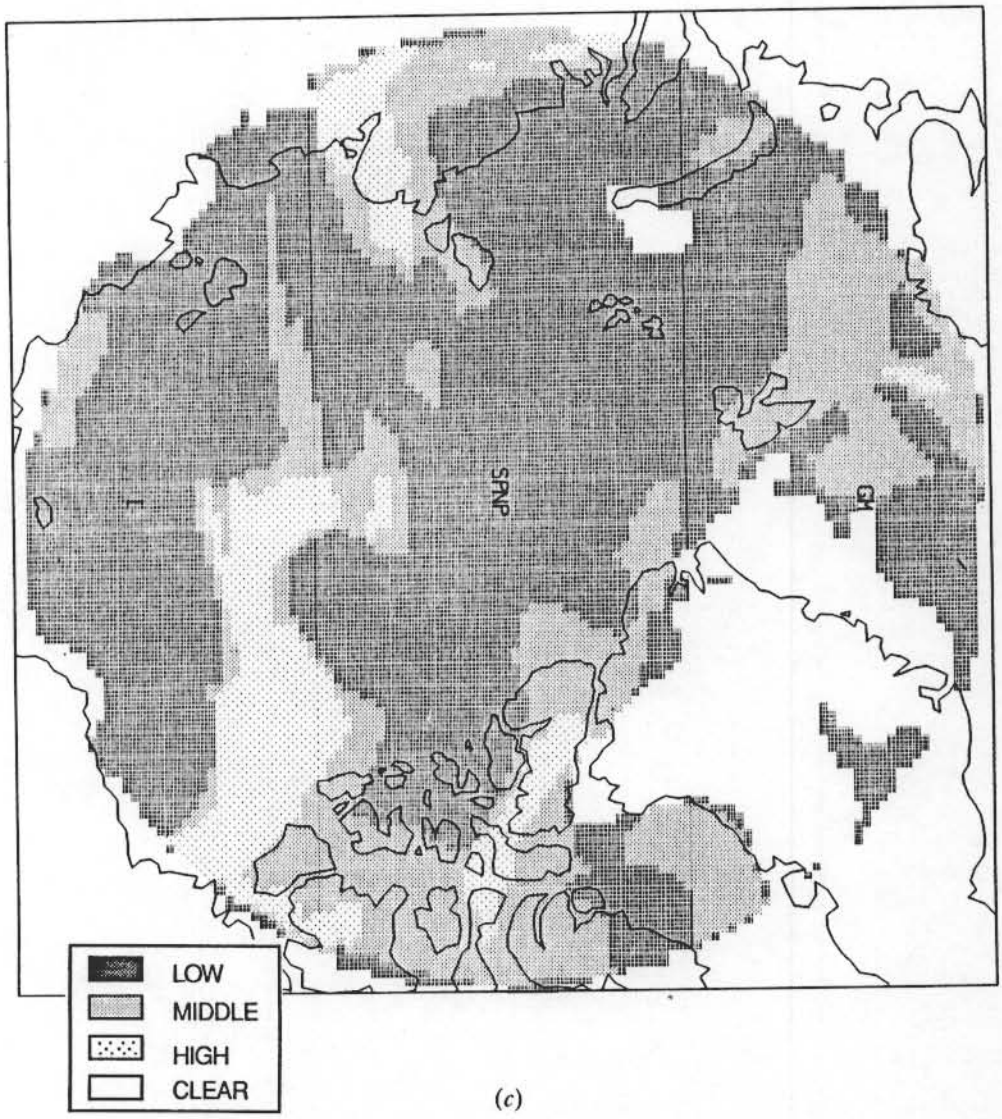
SPNP
LOW
MIDDLE
HIGH
CLEAR

(*c*)

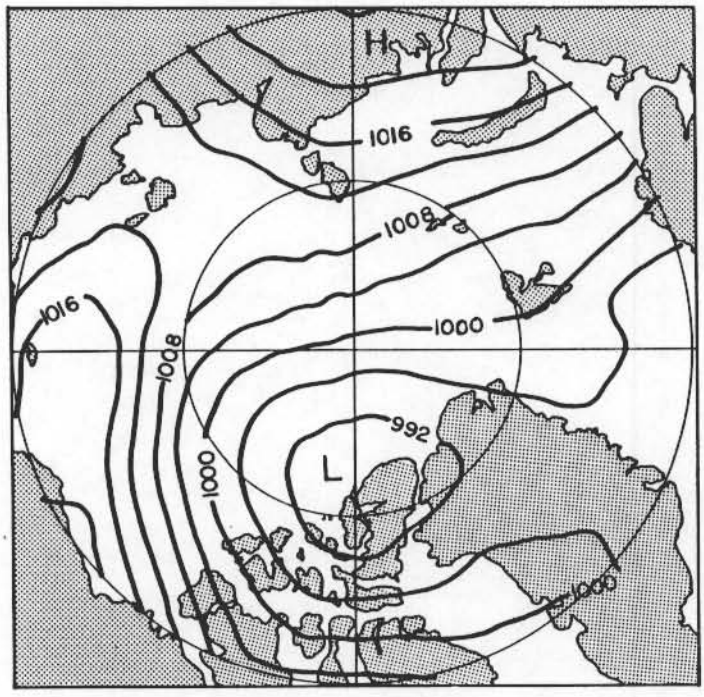
H
1016
1008
1000
992
L
1016
1008
1000

(*d*)

**Acknowledgments**

This work was supported by NASA grants NAG-5-417 and NAG-5-898 to the University of Colorado, Boulder, and by the U.S. Department of Energy, $CO_2$ Research Division, agreement DE-ACO2-81EV10665 and U.S. Air Force grant 86-0053 to Columbia University, New York. K.McG. wishes to acknowledge the sponsorship of the United States Air Force under grant AFOSR-86-0195. We thank Margaret Strauch for word processing support and Maria Neeri for drafting some of the figures.

**References**

ASTAPENKO, P. D., 1960, *Atmospheric Processes in the High Latitude of the Southern Hemisphere*, Section 2 of the IGY Program (Meteorology) 3, Academi Nauk SSSR, (translators Israel Program for Scientific Translations, Jerusalen), p. 286.

BARRY, R. G., CRANE, R. G., ANDERSON, M. R., CARLETON, A. M., and SCHARFEN, G., 1984 a, Empirical analysis of cryosphere-cloud interactions. In *Cryosphere-Cloud Interactions near the Snow/Ice Limit*, edited by R. G. Barry, K. P. Shine and A. Henderson-Sellers, CIRES, (Boulder: University of Colorado), p. 75.

BARRY, R. G., CRANE, R. G., NEWELL, J. P., and SCHWEIGER, A., 1986, Empirical and modeled synoptic cloud climatology of the Arctic Ocean. Final Report to NASA, NAG-5-417, Cooperative Institute for Research in Environmental Sciences, University of Colorado, Boulder, p. 103.

BARRY, R. G., CRANE, R. G., SCHWEIGER, A., and NEWELL, J., 1987, Arctic cloudiness in spring from satellite imagery. *J. Clim.*, 7 (in the press).

BARRY, R. G., HENDERSON-SELLERS, A., and SHINE, K. P., 1984 B, Climate sensitivity and the marginal cryosphere. In *Climate Processes and Climate Sensitivity* (Geophysics Monograph 29) edited by J. E. Hansen and T. Takahashi, (Washington D.C.: American Geophysical Union), p. 221.

BERLYAND, T. G., and STROKINA, L. A., 1980, *Global Distribution of Total Cloud Amount* (in Russian) (Leningrad: Gidrometeoizdat), p. 72.

CARLETON, A. M., 1984, Cloud–cryosphere interactions. In *Satellite Sensing of a Cloudy Atmosphere*, edited by A. Henderson-Sellers (London: Taylor and Francis), p. 289.

CRANE, R. G., and BARRY, R. G., 1984, The influence of clouds on climate with a focus on high latitude interactions. *J. Clim.*, **4**, 71.

FRASER, D. B., 1973, Synoptic weather patterns over the Arctic. In *Arctic Operational Meteorology*, edited by H. P. Wilson (Edmonton, Alberta: Environment Canada, Arctic Weather Central), p. 348.

FYE, F. K., 1978, The AFGWC automated cloud analysis mode. AFGWC-TM-100c-1978, Air Force Global Weather Central, Offutt, Nebraska, p. 97.

GORSHKOV, S. G. (editor), 1983, *World Ocean Atlas*, Vol. 3, *Arctic Ocean*, (Oxford: Pergamon Press).

HENDERSON-SELLERS, A., HUGHES, N. A., and WILSON, M., 1981, Cloud cover archiving on a global scale: a discussion of principles. *Bull. Am. met. Soc.*, **62**, 1300.

HUGHES, N. A., 1984, Global cloud climatologies: a historical review. *J. Climate appl. Met.*, **23**, 724.

HUGHES, N. A., and HENDERSON-SELLERS, A., 1985, Global 3-D nephanalysis of total cloud amount—climatology for 1979. *J. Climate appl. Met.*, **24**, 669.

HUSCHKE, R. E., 1969, Arctic cloud statistics from 'air-calibrated' surface weather observations. RAND Corporation Memo RM-6173-PR, Santa Monica, California, p. 79.

KUKLA, G. J., 1984, Variation of Arctic cloud cover during summer 1979, Part 1. Technical Report LDGO-84-2, Lamont-Doherty Geological Observatory of Columbia University.

LEDREW, E. F., 1987, Q-Vector analysis of five depression systems with the Polar Basin. *J. Clim.*, (submitted).

LOEWE, F., 1935, Das Klima des Grönlandischen Inlandeises. In *Handbuch der Klimatologie*, edited by W. Koppen and R. Grieger, 2, K, (Berlin: Borntraeger), p. 67.

MACDONALD, W. F., 1938, *Atlas of Climatic Charts of the Oceans* (Washington, D.C.: Weather Bureau, U.S. Department of Agriculture).

McGuffie, K., 1985, Cloud and radiation over cryospheric surfaces: climatology and climate sensitivity. Ph.D. thesis, University of Liverpool, Liverpool, England, p. 363.

Malberg, H., 1973, Comparison of mean cloud cover obtained by satellite photographs and ground-based observations over Europe and the Atlantic. *Mon. Weath. Rev.*, **101**, 893.

Putnins, P., 1970, The climate of Greenland. In *Climates of the Polar Regions* (*World Survey of Climatology*, Vol. 14), edited by S. Orvig, (Amsterdam: Elsevier), p. 3.

Robinson, D. A., Kukla, G. J., and Serreze, M., 1985, Arctic cloud cover during the summer of 1977–1979. Technical Report LDGO-85-5, Lamont-Doherty Geological Observatory of Columbia University, Palisades, New York, p. 175.

Robinson, D. A., Kukla, G. J., and Serreze, M., 1986a, Arctic summer cloudiness. *Proceedings of the Sixth Conference on Atmospheric Radiation* (Boston: American Meteorological Society), p. 176.

Robinson, D. A., Scharfen, G., Serreze, M. C., Kukla, G., and Barry, R. G., 1986b, Snow melt and surface albedo in the Arctic Basin. *Geophys. Res. Lett.*, **13**, 945.

Schiffer, R. A., and Rossow, W. A., 1983, The International Satellite Cloud Climatology Project (ISCCP). The first project of the World Climate Research Programme. *Bull. Am. met. Soc.*, **64**, 779.

Sherr, P. E., Glasser, A. M., Barnes, J. C., and Willard, J. M., 1968, World-wide cloud distribution for use in computer simulations. Final Report Contract NAS-8-21040, Allied Research Associates, Inc., Baltimore, Maryland, p. 272.

Shine, K. P., and Crane, R. G., 1984, The sensitivity of a one-dimensional thermodynamic sea ice model to a change in cloudiness. *J. geophys. Res.* C, **89**, 10,615.

Tanizer, T., 1968, Differences between cloud coverages observed from ground stations and satellites. *Időjárás*, **72**, 321.

Thorndike, A. S., and Colony, R., 1980, Arctic Ocean Buoy Program. Data Report. 19 January 1979–31 December 1979. Polar Science Center, University of Washington, Seattle, p. 131.

Voskresenskiy, A. T., and Chukanin, K. I., 1959, Meteorologicheskie usloviya obledeneniya v oblakov tipa *st* i *sc*. *Arkt. Antarkt. Nauch-Issled. Inst., Trudy*, **228**, 124.

Vowinckel, E., 1962, Cloud amount and type over the Arctic. *Publications in Meteorology*, No. 51 (Montreal: Arctic Meteorology Research Group, McGill University), p. 27.

World Meteorological Organization, 1956, *International Cloud Atlas* (Geneva: WMO).